

Dihydropyridinone Alkaloid Artifacts from *Curcuma longa* and their Anti-Migration Activity Against HepG2 Cells

Fatma M. Abdel Bar*

Pharmacognosy department, Faculty of pharmacy, Mansoura University, Mansoura 35516, Egypt

(Received August 22, 2015; Revised November 08, 2015; Accepted November 11, 2015)

Abstract: A new 2,3-dihydropyridin-4(1H)-one alkaloid (**2**), and two other known derivatives (**1** and **3**) were isolated from *Curcuma longa*. The isolated alkaloids are shown to be artifacts formed during extraction procedure. Three new (**2**, **5** and **7**) and two known (**4** and **6**) methoxylated compounds were derived from **1** and **3**. Structures were assigned using IR, HRESIMS analyses and 1 and 2D NMR spectroscopy. The anti-migration and anti-proliferation activities against the hepatocellular carcinoma cells, HepG2 were investigated. Compounds **3** showed remarkable anti-migration activity at 40 μ M (absolute migration capability, $MC_A = -7.4 \times 10^{-4}$ mm/h). The methylated derivatives **4** showed pronounced anti-migration activity ($MC_A = -4.9 \times 10^{-4}$ mm/h) compared to its parent compound **1** ($MC_A = 1.49 \times 10^{-3}$ mm/h) at 20 μ M. The dihydropyridinone derivatives were shown to develop actin stress fibres in treated HepG2 cells which may indicate its role in cell migration inhibition. Compared to curcumins I, II and III, the obtained dihydropyridinone analogues showed lower anti-proliferative activity.

Keywords: *Curcuma longa*; dihydropyridinone alkaloids; anti-migration; Curcumin; HepG2 cells. © 2016 ACG Publications. All rights reserved.

1. Introduction

Curcuminoids isolated from *Curcuma longa* L., have been shown to possess various pharmacological effects [1, 2]. Due to the importance of this group of compounds, many derivatives were synthesized. Interestingly, a series of new 2-aryl-6-styryl-2,3-dihydropyridin-4(1H)-ones derivatives were obtained by treatment of curcuminoids with aq. NH_3 [3]. Additionally, a series of *N*-alkyl and *N*-aryl 2,3-dihydro-4-pyridinones have been reported from the reaction of curcumin and bis-demethoxycurcumin with primary amines using microwave-assisted synthesis [4–7], and have been tested for their antitumor activity against several cell lines using MTT assay [8].

Hepatocellular carcinoma is one of the most common lethal cancers in the world [9]. Inhibiting cell migration and invasion is critical in the treatment procedure of hepatocellular carcinoma. Scratch wound healing assay is a convenient and inexpensive method for high throughput analysis of cell migration *in vitro* [10]. In the current study 2,3-dihydro-4-pyridinone derivatives (**1-3**) were simply obtained as artifacts during the routinely acid-base extraction procedure of powdered turmeric. Additionally, four methylated products (**4-7**) were derived. The potential anti-metastatic activity of the obtained compounds (**1-7**) along with curcumins I, II and III were investigated against the

* Corresponding author: E-Mail: fatma_maar@yahoo.com; Phone: +20 1007536700 Fax: +20 50 2247496

hepatocellular carcinoma (HepG2) cells using scratch wound healing assay. Moreover, the antiproliferative activity against HepG2 cells was evaluated using MTT colorimetric assay.

2. Materials and Methods

1.1. General experimental information

BRUKER Avance III spectrometer, 400 MHz for ^1H -NMR and 100 MHz for ^{13}C -NMR, spectra were obtained in DMSO- d_6 , Acetone- d_6 or CDCl_3 solutions with TMS as internal standard. Melting points were determined on Stuart[®] melting point apparatus model SMP10. High-resolution ESIMS experiments were conducted using a JEOL JMS-T100 LP AccuTOF LC-Plus equipped with an ESI source (JEOL Co. Ltd, Tokyo, Japan). EI-MS analyses were obtained using a Thermo Scientific DSQ[™] II instrument. IR spectra were acquired using Thermo Scientific Nicolet[™] iS[™]10 FT-IR spectrometer instrument. TLC is performed on precoated silica gel 60 GF₂₅₄ (Merck, Germany). Silica gel G 60-230 mesh (Merck[®], Germany) and reversed phase C₁₈ silica gel (BAKERBOND[®], USA) were used for column chromatography. For monitoring and investigation of cell lines and for wound healing assay inverted microscope (Olympus CKX41, Tokyo, Japan) was used. For MTT assay: the optical density (OD) was measured at 540 nm on BioTeck[®] microplate reader and CO₂ incubator (SHEL LAB) was used, SHEL DON[®] manufacturing Inc. All chemicals used were of reagent grade and obtained from commercial suppliers.

1.2. Plant materials

Rhizome of *Curcuma longa* L. was purchased at an herbal market in Mansoura, Egypt in October 2012 and the botanical authentication was done by Prof. Ibrahim Mashaly, Systematic Botany Department, Faculty of Sciences, Mansoura University. A voucher specimen was deposited in the herbarium of the college of pharmacy, Mansoura University (012-Mansoura-1).

1.3. Isolation and purification

Three kilograms of powdered dried rhizomes of *Curcuma longa* L. were defatted with *n*-hexane (4 X 5 L), soaked in NH_4OH (33%, Specific gravity 0.91 $\text{g}\cdot\text{mL}^{-1}$) – methanol, (1:4 v/v) for 24 h then extracted with methanol (3 X 5 L). The combined methanol extract was then concentrated under vacuum. The formed alkaloids were then purified using successive acid-base extraction by the addition of (dil.) HCl solution and shaking with EtOAc to remove pigments and impurities. The aqueous solution was then alkalized with NH_4OH , extracted with EtOAc and concentrated under vacuum to yield a crude alkaloidal residue (20 g). The obtained residue was purified as illustrated in Figure 1, monitored using silica gel TLC plates, CH_2Cl_2 - MeOH, 9:1 v/v as the solvent system and Dragendorff's reagent for visualization, to afford compounds **1** (R_f :0.62), **2** (R_f :0.52) and **3** (R_f :0.42), respectively.

1.4. Preparation of compounds 4-7 [11]

Dry potassium carbonate (6.9 mg, 0.05 mmol) was added to 1 equiv. (0.05 mmol) of **1** or **3** (18.5 mg or 15.5 mg, respectively) in dry acetone (1 mL), in each case separately. Methyl Iodide (14.2 mg, 0.1 mmol, 2 equiv.) was dissolved in 1 mL dry acetone and added dropwise. The reaction mixture was stirred for 24 h at room temperature, and then the reaction was stopped by addition of water. Acetone was removed and the product was extracted using CH_2Cl_2 (3 x 3 mL) and concentrated under reduced pressure. TLC of the crude reaction mixture revealed the presence of two products in each case.

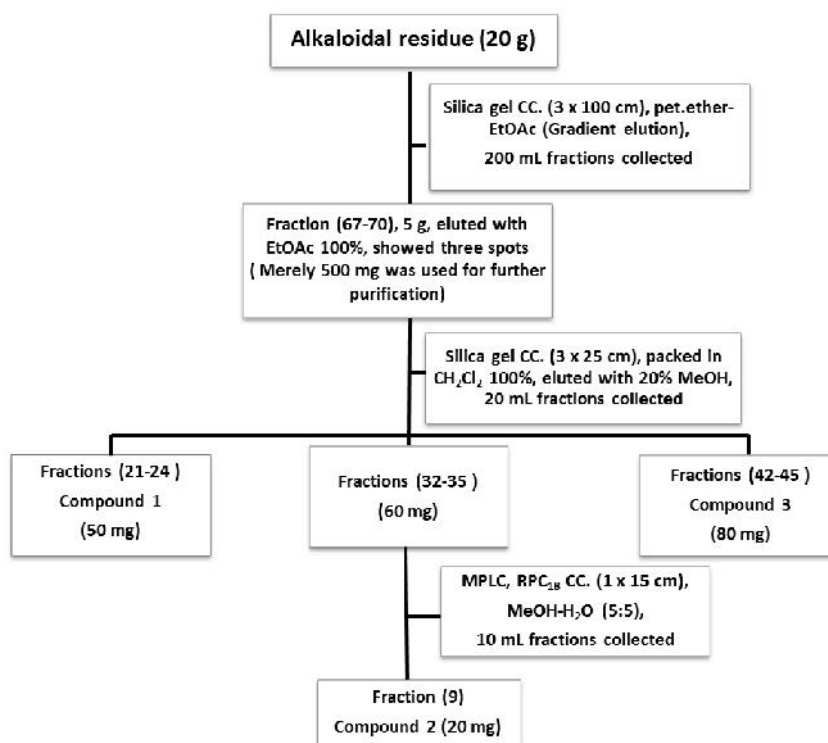


Figure 1. Purification procedure of compounds 1-3.

1.5. Purification of compounds 4-7

Briefly, the methylation product in each case was purified over silica gel CC. (15 x 1cm i.d.) packed in CH_2Cl_2 (100%) and eluted with MeOH (2% v/v) and 5 mL fractions were collected. In case of compound 1, fraction (20) afforded compound 4, 8 mg, R_f : 0.46 and fractions (22-23) afforded compound 5, 6 mg, R_f : 0.42 [TLC solvent system: CH_2Cl_2 - MeOH, 9:1 v/v]. While in case of compound 3, fraction (4) afforded compound 6, 10 mg, R_f : 0.55 and fractions (6-10) afforded compound 7, 12 mg, R_f : 0.48 using the same formerly mentioned solvent system.

1.6. Cell culture

Human hepatocellular carcinoma cell line HepG2 (ATCC No. HB-8065) was purchased from American Type Culture Collection (ATCC, Rockville, MD, USA).

1.7. Scratch wound healing anti-migration assay [10, 12]

HepG2 cells were seeded in 24-well plates at 1×10^4 cells/well and cultured in DMEM containing 10% FBS for 72 h to reach >90% confluence. Confluence cells were scrapped using a sterile 200 μL pipette tip along the diameter of the well. The cell debris was discarded by washing with PBS then replaced with 500 μL of media containing 1% DMSO (negative control) or test compound 40, 20 and 10 μL (dissolved in not more than 1% DMSO and diluted with DMEM). Resveratrol was used as the positive control [13]. Wound closure of the cells was observed under the microscope at magnification 10X, and photographs were captured immediately after treatment (0 h) and 48 h later. Duplicate of wells were used for each concentration and three fields of the wounds were captured and mean values were analyzed. Absolute migration capability (MC_A) was applied to measure the migration capability of HepG2 cells after treatment [14].

$$MC_A \text{ (mm/h)} = \frac{G_0 - Gt}{2t}$$

Where G_0 is the initial gap (mm) for the cell line at 0 h, Gt is the final gap (mm) for the cell line treated with test compound at certain concentration or vehicle alone for a time period of t (h) and t is the overall time period for incubation (h).

1.8. MTT anti-proliferation assay [15, 16].

HepG2 cells were plated in 96-well plates at an initial density of (1×10^4) cells/100 μ L/well). After 24 h incubation, the cells were treated with tested compounds (100, 40, 20 and 10 μ M) in triplicates. After incubation for 48 h, 20 μ L of MTT were added to each well and further incubated for 3 h at 37 $^{\circ}$ C. Subsequently, the medium was removed and 100 μ L isopropyl alcohol containing 0.04 N HCl were added to each well to dissolve the formed formazan crystals of the viable cells, and the solubilized formazan product was quantified by the use of a microtiter plate reader at 540 nm. The percentage cell viability was calculated from: % cell viability = (average absorbance of treated cells / average absorbance of control cells) \times 100. The experimental data were processed by means of Microsoft Excel software. Results are presented as means \pm standard errors of three independent experiments.

1.9. Statistical analysis

Data in scratch wound healing assay were presented as mean values \pm standard error of the mean (SEM).

3. Results and Discussion

3.1. Structure elucidation

APT spectrum of compound **2** revealed the presence of 18 carbon signals and suggested the presence of two aromatic rings with different environment. A symmetric *para*-substituted phenyl ring was suggested from two proton doublets at δ_H 6.85 ($J=8.8$ Hz, 2H) and 7.33 ($J=8.8$ Hz, 2H) assigned for H-2'/6' and H-3'/5', respectively. Another aromatic ring with an ABX substitution pattern was revealed from the proton doublets at δ_H 7.26 ($J=2.0$ Hz, H-2''), δ_H 6.84 ($J=8.0$ Hz, H-5'') and δ_H 7.03 ($J=8.0, 2.0$ Hz, H-6''). Additionally, a non-substituted *Trans* double bond was suggested from two doublets ($J=16.4$ Hz) at δ_H 6.68 (H-8'') and 7.35 (H-7''). This double bond was assumed to be attached to the tri-substituted aromatic ring to give a styryl moiety. HMBC correlation of the proton H-2'' and H-6'' with the carbon signal at δ_C 134.5 (C-7'') confirmed this assumption. However, the remaining resonances at δ_C 190.8 (C=O), 158.3 (C), 99.1 (CH), 57.3 (CH) and 44.5 (CH₂) were the most characteristic signals and suggested a hetero ring system. A highly deshielded signal at δ_C 158.3 (C-6) suggested its attachment to a hetero-atom however; the unexpected upfield shift of C-2 (57.3 ppm) indicated its attachment to nitrogen and not to an oxygen atom. This deshielded carbon (C-6) was confirmed to be attached to the styryl moiety at C-8'' from HMBC correlation of H-7'' and H-8'' with C-6. ¹H-NMR spectrum showed a singlet proton at δ_H 5.20 and three doublet of doublets at δ_H 4.70 (H-2, $J=13.2, 4.4$ Hz), 2.36 (H-3_{eq}, $J=16.0, 4.8$ Hz) and 2.57 (H-3_{ax}, $J=15.6, 15.6$ Hz) each has integral of one proton. Thus, a 2,3-dihydro-4-pyridinone structure was suggested for the third ring system. The linkage of the *para*-hydroxy phenyl moiety to C-2 was proved through HMBC correlations (Figure 2B). HRESIMS that showed peak at m/z 338.13863 (M+H)⁺, {Calcd. for C₂₀H₁₉NO₄ 338.13923} confirmed the deduced structure. Therefore, compound **2** was established to

be a new structure, namely (*E*)-6-(4''-hydroxy-3''-methoxystyryl)-2-(4'-hydroxyphenyl)-2,3-dihydropyridin-4(1*H*)-one.

Compound **1** was established to be the known structure, namely (*E*)-2-(4'-hydroxy-3'-methoxyphenyl)-6-(4''-hydroxy-3''-methoxystyryl)-2,3-dihydropyridin-4(1*H*)-one (Huo et al., 2009). Similarly, compound **3** was established to be the known structure, namely (*E*)-2-(4'-hydroxyphenyl)-6-(4''-hydroxystyryl)-2,3-dihydropyridin-4(1*H*)-one (Huo et al., 2009).

Elucidation of the conformation of the six-membered azahexene ring in compounds **1-7** was determined based on the *J*-value of H-2 with the methylenic protons H-3_{ax,eq} [17], Figure 2C. Therefore, an axial orientation was confirmed for the proton H-2 and an equatorial position for the phenyl ring at C-2. This result is consistent with the fact that the bulkier group tend to be in the equatorial position for more stability [18].

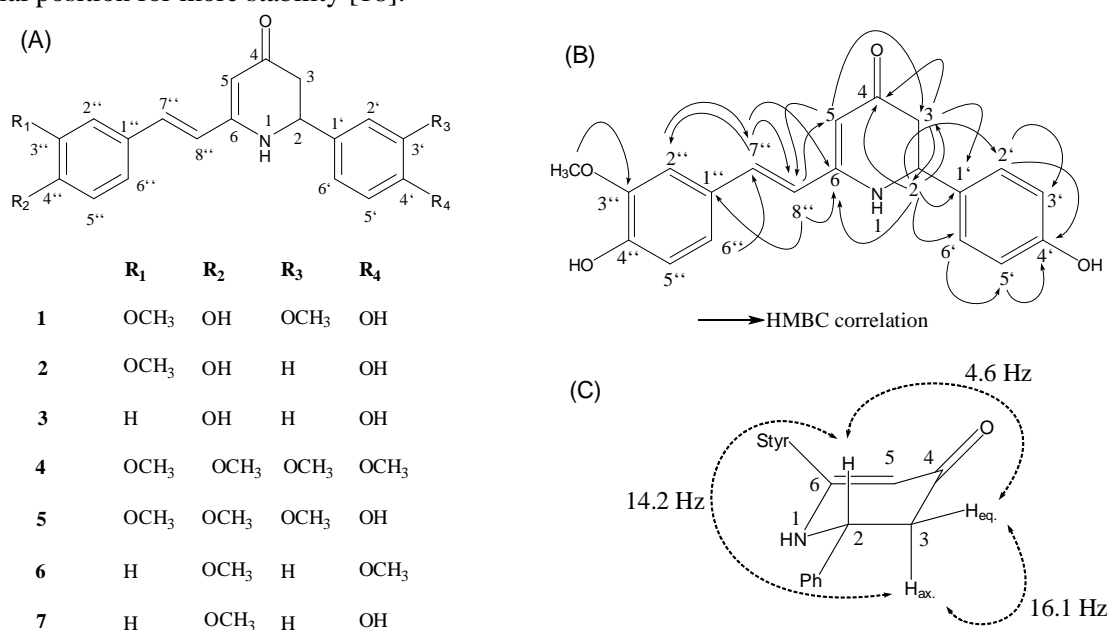


Figure 2. (A) Chemical structures of compounds **1-7**; (B) some important HMBC correlations of compound **2**; (C) Conformational analysis of the six-membered azahexene ring of the dihydropyridinones (**1-7**) with *J* values calculated by averaging.

It is worth noted that compounds **1-3** are suggested to be formed as artifacts during the extraction procedure as a result of reaction between curcumins I, II and III with ammonium hydroxide solution. The proposed mechanism for this reaction is published before [3]. To prove such hypothesis, the extraction procedure was repeated using Na₂CO₃ however, no alkaloids were produced. Consequently, compound **2** is supposed to be formed from demethoxycurcumin (curcumin II).

Methylation of **1** and **3** afforded two new compounds **5** and **7** and two other known methylated derivatives **4** and **6** [3].

Compound **5**, prepared by methylation of **1**, is a more polar product than **4** and showed HRESIMS showed peak at *m/z* 382.16500 (M+H)⁺, {Calcd. for C₂₂H₂₃NO₅ 382.16545} and indicated a tri-methoxylated product. ¹H-NMR spectrum of **5** showed three singlets at δ_H 3.84, 3.85 and 3.86 each has an integral of 3H indicated the presence of three methoxyl groups. This was confirmed from APT spectrum that showed three methyl resonances at δ_C 56.0-56.1. The position of the introduced methoxyl group was assigned to C-4'' based on the upfield shift of C-5'' (-4.9 ppm) compared to that of compound **1**. Additionally, the proton doublet H-5'' (δ_H 6.78, *J* = 8.0 Hz) appeared more shielded than other aromatic protons and showed HMBC correlations with the carbon signals at δ_C 128.0 (C-1''), 150.6 (C-3'') and 121.6 (C-6'') confirming their assignments. Thus, compound **5** was established to be a new compound namely (*E*)-6-(3'',4''-dimethoxystyryl)-2-(4'-hydroxy-3'-methoxyphenyl)-2,3-dihydropyridin-4(1*H*)-one.

Compound **7**, prepared by methylation of **3**, is a more polar product than **6** and showed HRESIMS peak at m/z 322.14396 ($M+H$)⁺, {Calcd. for C₂₀H₁₉NO₃ 322.14432} and indicated a mono-methoxylated product. ¹H-NMR of **7** showed a proton singlet at δ_H 3.76 with an integral of three protons confirming the presence of one methoxyl group. The methoxyl group was assigned to position C-4'' based on upfield shift (-1.9 ppm) of the carbon signal C-3''/5'' compared to that of compound **3** and the upfield shift (-2.9 ppm) of the carbon signal C-4' bearing a free OH group. Additionally, this methoxy signal showed ³J-HMBC correlation with the carbon signal at δ_C 160.9 (C-4''). Also, the proton doublet at δ_H 7.33 ($J=8.8$ Hz, H-2''/6'') showed HMBC correlation with the carbon signals at 134.4 (C-7'') and 160.9 (C-4'') and indicated that this methoxyl group belongs to the styryl moiety. All protons and carbons assignments of **7** were confirmed using HMBC correlations. Thus, compound **7** was established to be a new compound namely (*E*)-2-(4'-hydroxyphenyl)-6-(4''-methoxystyryl)-2,3-dihydropyridin-4(1*H*)-one.

Table 1. ¹H-NMR of compounds **2**, **5** and **7** (at 400 MHz, ^a in Acetone-d₆, ^b in CDCl₃, δ in ppm, J in Hz).

Position (H)	2 ^a	5 ^b	7 ^b
2	4.70, 1H, dd (13.2, 4.4)	4.61, 1H, dd (16.0, 4.0)	4.62, 1H, dd (14.4, 4.8)
3 _{eq.}	2.36, 1H, dd (16.0, 4.8)	2.46, 1H, dd (16.0, 4.0)	2.45, 1H, dd (16.4, 4.8)
3 _{ax.}	2.57, 1H, dd (15.6, 15.6)	2.66, 1H, dd (16.0, 16.0)	2.67, 1H, dd (16.4, 14.4)
4	---	---	---
5	5.20, 1H, s	5.29, 1H, s	5.30, 1H, s
6	---	---	---
1'	---	---	---
2'	6.85, 2H, d (8.8)	6.88, 2H, s	7.21, 2H, d (8.4)
3'	7.33, 2H, d (8.8)	---	6.81, 2H, d (8.8)
4'	---	---	---
5'	7.33, 2H, d (8.8)	6.90, 1H, d (8.0)	6.81, 2H, d (8.8)
6'	6.85, 2H, d (8.8)	6.91, 1H, dd (8.0, 2.0)	7.21, 2H, d (8.4)
1''	---	---	---
2''	7.26, 1H, d (2.0)	6.88, 2H, s	7.33, 2H, d (8.8)
3''	---	---	6.82, 2H, d (8.8)
4''	---	---	---
5''	6.84, 1H, d (8.0)	6.78, 1H, d (8.0)	6.82, 2H, d (8.8)
6''	7.03, 1H, dd (8.0, 2.0)	6.95, 1H, dd (8.0, 2.0)	7.33, 2H, d (8.8)
7''	7.35, 1H, d (16.4)	6.87, 1H, d (16.0)	6.90, d (16.4)
8''	6.68, 1H, d (16.4)	6.35, 1H, d (16.0)	6.34, 1H, d (16.4)
-NH-	6.47, brs	4.89, brs	5.00, brs
-OCH ₃	3.89, 3H, s	3.84, 3H, s	3.76, 3H, s
-OCH ₃	---	3.85, 3H, s	---
-OCH ₃	---	3.86, 3H, s	---
-OH	9.20, brs	---	---
-OH	9.50, brs	---	---

Table 2. APT data of compounds **2**, **5** and **7** (at 100 MHz, ^a in Acetone-d₆, ^b in CDCl₃, δ in ppm).

Position (C)	2 ^a	5 ^b	7 ^b
2	57.3 (CH)	58.6 (CH)	57.9 (CH)
3	44.5 (CH ₂)	44.5 (CH ₂)	44.1 (q)
4	190.8 (q)	192.9 (q)	193.2 (q)
5	99.1 (CH)	101.0 (CH)	100.2 (CH)
6	158.3 (q)	157.9 (q)	158.6 (q)
1'	132.2 (q)	132.9 (q)	131.6 (q)
2'	128.1 (CH)	109.2 (CH)	128.2 (CH)
3'	115.3 (CH)	146.9 (q)	116.1 (CH)
4'	157.2 (q)	146.0 (q)	156.8 (q)
5'	115.3 (CH)	114.7 (CH)	116.1 (CH)
6'	128.1 (CH)	120.0 (CH)	128.2 (CH)
1''	128.0 (q)	128.0 (q)	128.1 (q)
2''	109.7 (CH)	109.2 (CH)	129.0 (CH)
3''	148.2 (q)	150.6 (q)	114.4 (CH)
4''	147.9 (q)	149.4 (q)	160.9 (q)
5''	115.2 (CH)	111.2 (CH)	114.4 (CH)
6''	121.8 (CH)	121.6 (CH)	129.0 (CH)
7''	134.5 (CH)	134.3 (CH)	134.4 (CH)
8''	120.5 (CH)	120.8 (CH)	120.5 (CH)
-OCH ₃	55.4 (CH ₃)	56.0 (CH ₃)	55.4 (CH ₃)
-OCH ₃	---	56.0 (CH ₃)	---
-OCH ₃	---	56.1 (CH ₃)	---
-OCH ₃	---	---	---

Compound 2: Yellow amorphous powder, m.p. 194-196 °C, IR_{max} (KBr) 3382, 2926, 1643, 1558, 1510, 1461, 1397, 1268, 1166, 1122 and 905 cm⁻¹ and HRESIMS at *m/z* 338.13863 (M+H)⁺, {Calcd. for C₂₀H₁₉NO₄ 338.13923}, 336.12138 (M-H)⁻, {Calcd. 336.12358} and 360.11996 (M+Na)⁺, {Calcd. 360.12118}.

Compound 5: Yellow amorphous powder, m.p. 145-148 °C, IR_{max} (KBr) 3357, 2957, 2930, 2839, 1576, 1511, 1458, 1424, 1343, 1264, 1138, 1024, 966 and 927 cm⁻¹ and HRESIMS at *m/z* 382.16500 (M+H)⁺, {Calcd. for C₂₂H₂₃NO₅ 382.16545}, 380.14677 (M-H)⁻, {Calcd. 380.14980} and 404.14629 (M+Na)⁺, {Calcd. 404.14739}.

Compound 7: Yellow amorphous powder, m.p. 195-198 °C, IR_{max} (KBr) 3303, 3083, 2990, 2926, 2892, 2831, 1640, 1604, 1564, 1499, 1408, 1359, 1280, 1172, 1114, 1032, 963 and 816 cm⁻¹ and HRESIMS at *m/z* 322.14396 (M+H)⁺, {Calcd. for C₂₀H₁₉NO₃ 322.14432}, 344.12555 (M+Na)⁺, {Calcd. 344.12626} and 665.26353 (2M+Na)⁺, {Calcd. 665.26276}.

3.2. Anti-migration and Anti-proliferation activity

Absolute migration capability (MC_A) was used as an evaluation parameter for the migration capability of HepG2 cells. MC_A value for untreated cells (negative control) was 4.23 x 10⁻³ mm/h at 48 h of incubation, which represented the migration capability of HepG2 cells in normal conditions. The untreated HepG2 cells (negative control) spread along the wound edges (gap distance at 0 h, 0.599 mm) and became highly colonised at 48 h (gap distance, 0.193 mm), Figure 3A. In the scratch wound assay, the largest gaps observed after treatment revealed the most effective anti-migration agent. Also, smaller value of MC_A expresses the lower migration capability. Negative MC_A values represented no migration capability of HepG2 cells. All compounds were tested at concentration of 40, 20 and 10 μM and MC_A was compared after 48 h of treatment. Based on the results in Table 2, compound **3**, **4**, curcumin I and curcumin II inhibited the migration capability of HepG2 cells. The highest anti-migration activity was observed for curcumin I (Figure 3B) at 40 μM (MC_A = -1.18 x 10⁻³ mm/h) compared to negative control. The new dihydropyridinone derivatives **3** (Figure 3C) showed marked anti-migration activity at 40 μM (MC_A = -7.4 x 10⁻⁴ mm/h). Among the prepared methylated dihydropyridinone derivatives, compound **4** (Figure 3D) showed pronounced anti-migration activity at 20 μM (MC_A = -4.9 x 10⁻⁴ mm/h) compared to its parent compound **1** (MC_A = 1.49 x 10⁻³ mm/h) at the

same concentration. Curcumin II (Figure 3E) showed anti-migratory activity at 40 μM ($MC_A = -4.69 \times 10^{-4}$ mm/h) comparable to that of **4** at lower concentration level (20 μM).

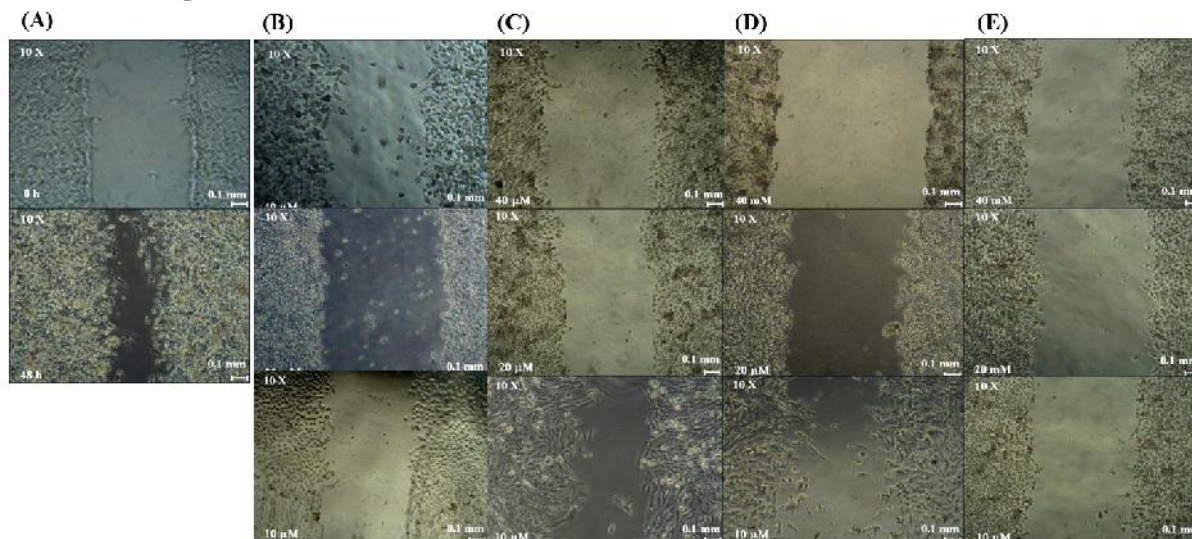


Figure 3. Images of the wounded layer of HepG2 cells (X 10); (A) Negative control at 0 and 48 h; (B) (C), (D) and (E) Compounds Cur-I, Cur-II, compound **3** and **4**, respectively at three concentration levels (40, 20 and 10 μM) after 48 h of treatment.

The new dihydropyridinone derivatives were observed to develop actin stress fibres in treated HepG2 cells (Figure 4). The relation between stress fibres and cell migration was reported before. It was observed that stress fibres are more prominent in stationary cells [19], suggesting that stress fibres inhibit cell migration [19].

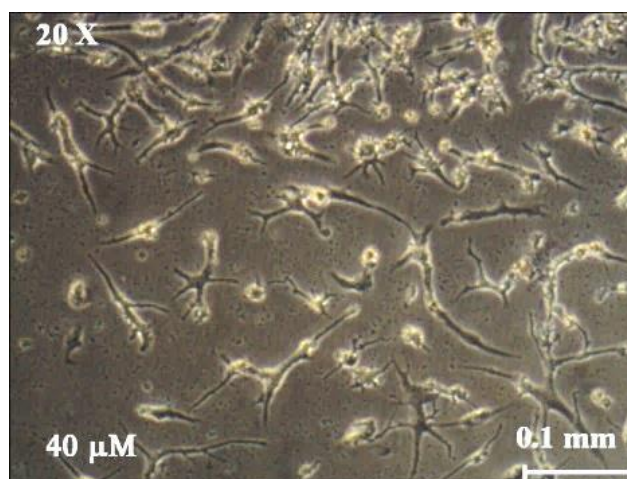


Figure 4. HepG2 cells (X 20) treated with compound **3** (40 μM) after 48 h of treatment showed actin stress fibres.

Table 3. Gap distances \pm standard deviation (mm) and absolute migration capability (MC_A mm/h) of compounds 1-7 and curcumins I, II and III against HepG2 cells measured using scratch wound healing assay using resveratrol as positive control and untreated wound (DMSO) as negative control.

Test compound	Concentration (μ M)	Gap distance (mm) \pm (SEM)	Absolute migration capability, MC_A (mm/h) after 48 h
Comp. 1	40	0.382 \pm 0.004	2.26 $\times 10^{-3}$
	20	0.459 \pm 0.035	1.49 $\times 10^{-3}$
	10	0.384 \pm 0.040	2.24 $\times 10^{-3}$
Comp. 2	40	0.396 \pm 0.050	2.11 $\times 10^{-3}$
	20	0.383 \pm 0.022	2.25 $\times 10^{-3}$
	10	0.420 \pm 0.027	1.86 $\times 10^{-3}$
Comp. 3	40	0.670 \pm 0.000	-7.40 $\times 10^{-4}$
	20	0.539 \pm 0.050	6.25 $\times 10^{-4}$
	10	0.507 \pm 0.00	9.58 $\times 10^{-4}$
Comp. 4	40	0.577 \pm 0.050	2.29 $\times 10^{-4}$
	20	0.646 \pm 0.009	-4.9 $\times 10^{-4}$
	10	0.591 \pm 0.020	0.83 $\times 10^{-4}$
Comp. 5	40	0.459 \pm 0.017	1.46 $\times 10^{-3}$
	20	0.56 \pm 0.018	4.06 $\times 10^{-4}$
	10	0.466 \pm 0.012	1.39 $\times 10^{-3}$
Comp. 6	40	0.242 \pm 0.048	3.72 $\times 10^{-3}$
	20	ND	ND
	10	0.338 \pm 0.027	2.72 $\times 10^{-3}$
Comp. 7	40	0.551 \pm 0.012	5.00 $\times 10^{-4}$
	20	ND	ND
	10	0.438 \pm 0.003	1.68 $\times 10^{-3}$
Cur-I	40	0.712 \pm 0.007	-1.18 $\times 10^{-3}$
	20	0.538 \pm 0.031	6.35 $\times 10^{-4}$
	10	0.49 \pm 0.009	1.14 $\times 10^{-3}$
Cur-II	40	0.644 \pm 0.017	-4.69 $\times 10^{-4}$
	20	0.519 \pm 0.025	8.33 $\times 10^{-4}$
	10	0.413 \pm 0.012	1.94 $\times 10^{-3}$
Cur-III	40	0.429 \pm 0.023	1.77 $\times 10^{-3}$
	20	ND	ND
	10	0.496 \pm 0.009	1.07 $\times 10^{-3}$
Resveratrol (positive control)	40	0.464 \pm 0.008	1.41 $\times 10^{-3}$
	20	0.407 \pm 0.022	2.00 $\times 10^{-3}$
	10	0.401 \pm 0.016	2.06 $\times 10^{-3}$
DMSO (Negative control)	1% v/v	0.193 \pm 0.047	4.23 $\times 10^{-3}$
DMSO after 0 h	1% v/v	0.599 \pm 0.017	0.00

The anti-proliferation activity of dihydropyridinone artifacts was evaluated in comparison to curcumins I, II and III using microculture tetrazolium assay (MTT). The results are represented as % cell viability (Figure 5). It was observed that most of the tested compounds showed anti-proliferation activity at the tested concentration range (100-10 μ M). However, the new dihydropyridinone derivatives showed lower anti-proliferative activity compared to curcumins I, II and III. These results may indicate that the dihydropyridinone derivatives exhibited better anti-migration activity with less cytotoxicity against the human hepatocellular carcinoma cells (HepG2) compared to the tested curcuminoids.

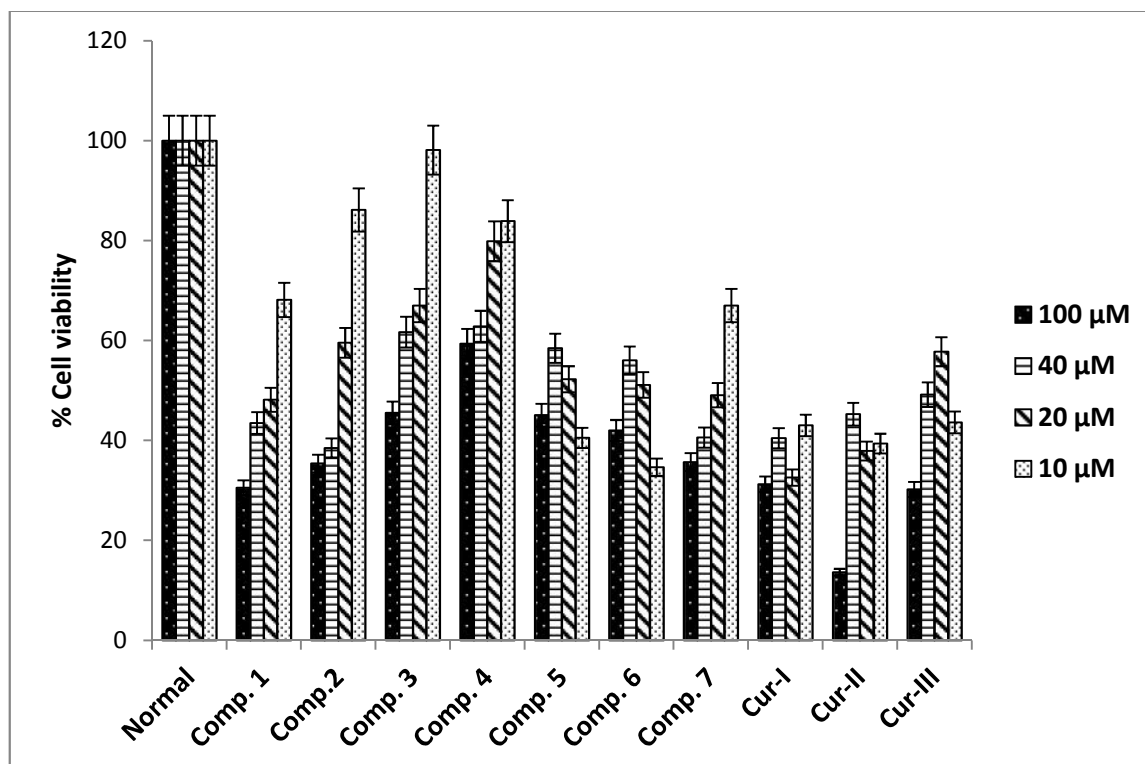


Figure 5. Anti-proliferation activity of compounds 1-7 and curcumins I, II and III against HepG2 cell line using MTT cell viability assay. Different concentrations of the tested compounds (100, 40, 20 and 10 μM) have been incubated for 48 h with cells and counted as percentage of untreated control, 0 μM (means \pm standard errors).

Acknowledgement

The author acknowledge Prof. Dr. Khalid A. El-Sayed, Prof. of Medicinal and Natural Product Chemistry, Department of Basic Pharmaceutical Sciences, College of Pharmacy, University of Louisiana at Monroe-USA, for his help in performing HRESIMS and Mr. Mohamed S. Abdel Razik, B.Ch. Faculty of Pharmacy, University of Mansoura, Egypt.

Supporting Information

Supporting Information accompanies this paper on <http://www.acgpubs.org/RNP>

References

- [1] H. J. Kim, H. S. Yoo, J. C. Kim, C. S. Park, M. S. Choi, M. Kim, H. Choi, J. S. Min, Y. S. Kim, S. W. Yoon and J. K. Ahn (2009). Antiviral effect of *Curcuma longa* Linn extract against hepatitis B virus replication, *J. Ethnopharmacol.* **124**, 189–196.
- [2] I. Chattopadhyay, K. Biswas, U. Bandyopadhyay and R. K. Banerjee (2004). Turmeric and curcumin: Biological actions and medicinal applications, *Curr. Sci.* **87**, 44-50.
- [3] Y. P. Huo, X. Qiu, W. Y. Shao, L. K. An, X. Z. Bu and L. Q. Gu (2009). Synthesis of new 2-aryl-6-styryl-2,3-dihydropyridin-4-(1H)-one derivatives from curcuminoids, *Chinese Chem. Lett.* **20(11)**, 1291-1295.
- [4] B. A. Saeed, R. S. Elias and W. A. Radhi (2010a). Microwave-Assisted Synthesis of Novel 2,3-Dihydro-4-Pyridinones, *Molecules* **15**, 8425-8430.
- [5] W. A. Radhi and B. A. Saeed (2010). The Investigation of ^1H NMR Spectra of 2,3-Dihydro-4-Pyridinones Derived from Bisdemethoxycurcumin, *Am. J. App. Sci.* **7(8)**, 1053-1056.

- [6] B. A. Saeed, Y. Kawkab, K. Y. Saour and R. S. Elias (2009). The investigation of NMR spectra of dihydropyridones derived from Curcumin, *ARKIVOC (xiii)*, 42-54.
- [7] R. S. Elias, B. A. Saeed, K. Y. Saour and N. A. Al-Masoudi (2008). Microwave-assisted synthesis of dihydropyridones from curcumin, *Tetrahedron Lett.* **49**, 3049–3051
- [8] B. A. Saeed, K. Y. Saour, R. S. Elias, N. A. Al-Masoudi and P. La Cola (2010b). Antitumor and quantitative structure activity relationship study for dihydropyridones derived from curcumin, *Am. J. Immunol.* **6**, 7-10.
- [9] H. B. El-Serag and K. L. Rudolph (2007). Hepatocellular carcinoma: epidemiology and molecular carcinogenesis, *Gastroenterol* **132**, 2557-2576.
- [10] C.-C. Liang, A.Y. Park and J.-L. Guan (2007). *In vitro* scratch assay: a convenient and inexpensive method for analysis of cell migration *in vitro*, *Nat. Protoc.* **2(2)**, 329-333.
- [11] J. Chao, H. Li, K.-W. Cheng, M.-S. Yu, R. C.-C. Chang and M. Wang (2010). Protective effects of pinostilbene, a resveratrol methylated derivatives, against 6-hydroxydopamine-induced neurotoxicity in SH-SY5Y cells, *J. Nutr. Biochem.* **21**, 482-489.
- [12] A. J. Chew, N. Z. Abidin and N. B. Abdul-Wahab (2012). Anti-proliferation and anti-migration activities of ten selected Zingiberaceae species against MDA-MB-231 cells, *J. Med. Plants Res.* **6(21)**, 3711-3723.
- [13] H.-B. Yu, D.-Y. Li, H.-F. Zhang, H.-Z. Xue, C.-E. Pan, S.-H. Zhao and L. Wang (2010). Resveratrol Inhibits Invasion and Metastasis of Hepatocellular Carcinoma Cells, *J. Anim. Vet. Adv.* **9(24)**, 3117-3124.
- [14] C. C. Peng, K. C. Chen, R. Y. Peng, C. C. Chyau, C. H. Su and H. M. Hsieh-Li (2007). *Antrodia camphorata* extract induces replicative senescence in superficial TCC, and inhibits the absolute migration capability in invasive bladder carcinoma cells, *J. Ethnopharmacol.* **109**, 93-103.
- [15] R. F. Hussain, A. M. E. Nouri and R. T. D. Oliver (1993). A new approach for measurement of cytotoxicity using colorimetric assay, *J. Immunol. Meth.* **160(1)**, 89-96.
- [16] T. I. Valyakina, R. L. Komaleva, E. E. Petrova, A. A. Malakhov, O. G. Shamborant, T. M. Andronova and V. A. Nesmeyanov (1998). Endogenous tumour necrosis factor-alpha sensitise melanoma cells to glucosaminylmuramyl dipeptide, *F.E.B.S. Lett.* **426**, 373-376.
- [17] M. Bruch (1996). NMR Spectroscopy Techniques, Second Edition, (Practical Spectroscopy) 2nd Edition, New York, Basel: Marcel Dekker Inc., USA, 249-250.
- [18] T.N. Sorrell (2005). Organic Chemistry, second ed. University Science Books Publication, p. 95.
- [19] Couchman, J.R., Rees, D.A., 1979. The behaviour of fibroblasts migrating from chick heart explants: changes in adhesion, locomotion and growth, and in the distribution of actomyosin and fibronectin, *J. Cell Sci.* **39**, 149-165.